Packaging effects on MEMS pressure sensor hysteresis

Packaging Effects on MEMS Pressure Sensor Hysteresis

Y. Hamid[1,2], D.A. Hutt[1], D.C. Whalley[1] and R. Craddock[2]
[1] Wolfson School of Mechanical, Electrical and Manufacturing Engineering, Loughborough University, Loughborough, Leicestershire, LE11 3TU, UK
[2] Druck Ltd a division of BHGE, 2 Fir Tree Lane, Groby, Leicestershire, LE6 0FH, UK
E-mail: y.hamid@lboro.ac.uk / youssef.hamid@bhge.com

Abstract

Micro-electro-mechanical systems (MEMS) have allowed high precision pressure sensors to be manufactured at low cost, but they typically exhibit some level of hysteresis behaviour, which is believed to be primarily due to the materials used to package them. In order to evaluate the effects of the different packaging materials and processes, in this study, the performance of piezoresistive absolute pressure MEMS was measured for each of the first two packaging stages of the product assembly process. Sensing elements first packaged in a "floating exposed" configuration and then in an "attached exposed" configuration were compared. These two different packaging configurations exhibited distinct hysteresis behaviour when thermally cycled. After applying a third order polynomial fit to the raw data, stabilized and moving hysteresis loops were observed for the floating exposed and attached exposed configurations respectively. The stabilized hysteresis is believed to originate from the inelastic behaviour of the die metallisation, whereas the non-stabilized behaviour stems from the adhesive used to attach the die to the housing.

Introduction

Pressure is an important parameter to monitor in many industrial processes, as well as in oil and gas, automotive and aircraft systems, etc. Druck Ltd. manufactures silicon-based piezoresistive absolute pressure sensors, for which a cross sectional schematic of the basic sensing element (SE) is shown in Fig. 1. Differential pressure between the internal pressure, P_{ref}, and that applied to the active face of the die induces a deflection of the silicon diaphragm. The deflection leads to a stress concentration at the top surface of the diaphragm where four strategically doped areas, that act as piezoresistors, experience high stress fields. Due to the piezoresistive effect [1,2], changes in the level of stress within the piezoresistors causes a change in their resistance. The piezoresistors are connected in a Wheatstone bridge configuration, where the resistance changes induce a variation in the bridge output voltage which is directly related to the external pressure. In addition to the piezoresistors, each die has a diode fabricated on its surface which is used as a temperature sensor based on its forward-bias voltage being proportional to temperature.

Mechanical properties [3], piezoresistive properties [1] and theoretical transduction models [4,5] of such piezoresistive pressure SEs are available in the literature. Packaging of the SE is necessary to enable it to operate as a pressure sensor whilst protecting it from harsh environments and connecting it to the required electronic instrumentation. However, sensor models seldom consider the packaging structure within which the SE is embedded [6]. This is understandable as models accounting for package elements would be specific to that particular combination of packaging elements and cannot be generalized. However, the predicted performance of the SE is incomplete without taking into account the effects of the package in which it is embedded.

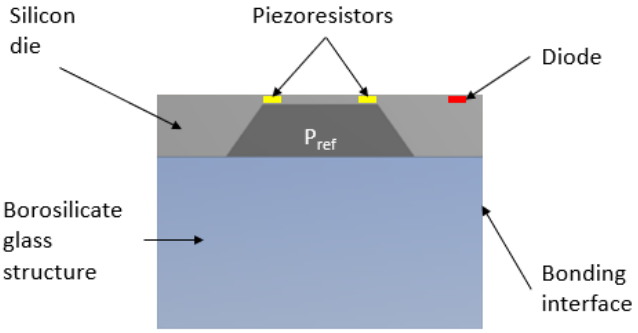

Fig. 1 The basic sensing element (SE) consisting of the silicon die bonded to a borosilicate glass structure

For low pressure applications, e.g. 50 to 200 kPa, a thin silicon diaphragm is required in order to provide sufficient sensitivity to pressure variation. However, temperature variations may result in packaging stresses that can be transferred to the piezoresistors which are comparable to the pressure-related stresses that the sensor is designed to measure. Despite the fact that the device is designed so that, as far as possible, any stresses affecting the piezoresistors are equal and are therefore cancelled out by the Wheatstone bridge, any non-symmetric stresses could be falsely misinterpreted as pressure inputs. Due to manufacturing tolerances and the required assembly sequences, packaging rarely has perfectly balanced effects on the Wheatstone bridge and any level of imbalance may not remain constant with time.

This study therefore investigated packaging effects as a main performance driver of the sensor's non-repeatability by comparing the behaviour of the same physical examples of typical SEs which were sequentially packaged in two different ways, as shown in Fig. 2. In the first instance, referred to as the "floating exposed" (FE) configuration, the SEs were wire bonded to the surrounding feedthroughs while allowed to float free. In the second instance, referred to as the "attached exposed" (AE) configuration, the SEs were again wire bonded, but also adhesively attached to the casing, as they would normally be in a fully packaged device. In this study, the same SEs that had been used for the FE configuration trials were repackaged for the AE tests allowing identification of any additional impacts on performance. The results presented here specifically focus on the thermally driven hysteresis behaviour of low pressure (50 to 200 kPa) absolute piezoresistive pressure sensors that were subjected to limited thermal cycling ranging from 5 to 65°C.

Thermal instabilities, as referred to by Liu et.al. [7], can be either repeatable or non-repeatable in nature. Repeatable instabilities can be caused, for example, by the non-linear thermal component of stress, that affects the thermal coefficient of resistance in silicon, or by the non-linear thermal component of the piezoresistive coefficient, which is dependent on the doping concentration [8]. These instabilities are repeatable in nature and can be eliminated if the sensing element's temperature is known during the measurement and a fitting function is applied to subtract the repeatable thermal contributions from the pressure signal. Non-repeatable instabilities such as package hysteresis effects are much more difficult to eliminate, and this paper therefore also focuses on establishing the benefit of fitting as a means of revealing different hysteresis behaviours as a result of the effect of packaging elements.

Packaging and testing methodology

A. Packaging scheme

To measure the bridge output and diode voltages, 38 µm diameter AlSi1% wires were ultrasonically bonded from the sensing element's bond pads to the stainless steel housing's feedthrough pins, as shown in Fig. 2. The wire bonding operation was achieved using a Kulicke and Soffa (K&S) wire bonder. Due to the SE's low mass (~7.5 mg), wire bonding could not be successfully completed without first anchoring the chip to provide it with mechanical support. The SE was therefore temporarily bonded to the housing using a standard commercial photoresist, which was initially left for 24h at room temperature. After that, the package was baked at 65°C for 30 minutes which attached the SE with sufficient mechanical strength to enable wire bonding to take place. Subsequent chemical removal of the photoresist was achieved by dissolving it away with acetone. Visual inspection of the final assembly was carried out to make sure the devices were clean and supported by the wire bonds only. Ten of these FE devices, as shown in Fig. 2(a), were successfully prepared in this way, for which the packaging elements affecting the diaphragm are solely the borosilicate glass, the metallisation bond pads and the wire bonds.

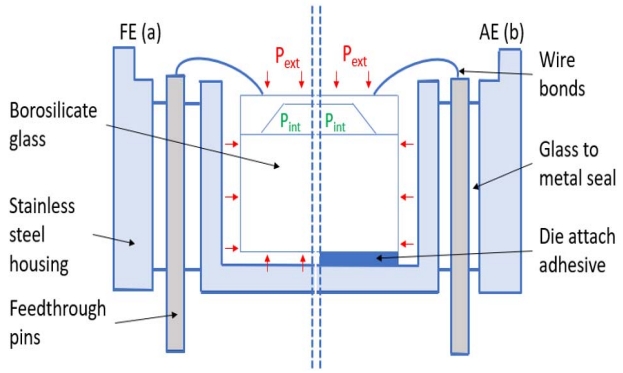

Fig. 2 Schematic of (a) "Floating Exposed" (FE) and (b) "Attached Exposed" (AE) packaging configurations

In the AE configuration, as shown in Fig. 2(b), the same ten units were re-packaged following the thermal and pressure cycling tests of the FE configuration. The re-packaging operation consisted of removing the existing wire bonds from the FE devices, adhesive bonding the SE to the housing using a standard two-part epoxy structural adhesive and wire bonding the die again to the feedthroughs. The SE was attached to the housing using a thin layer (~50 µm) of the pre-mixed epoxy adhesive and left to cure at room temperature for a minimum of 24 h. Only five of the original SE units were successfully re-packaged in this way, due to wire bonding difficulties on the remaining parts. However, by achieving this, the additional packaging elements that might affect the SE, in comparison with the FE configuration, were the structural adhesive and the stainless-steel housing. Any observed difference in hysteresis behaviour could therefore be attributed to these additional packaging elements combined with the previous thermal and pressure cycling effects.

B. Test equipment and profile

The sensors under test were mounted on connectors that were linked by a metal manifold capable of housing up to 12 sensors, as shown in Fig. 3. As only 10 sensors were tested the remaining positions available on the manifold were blanked off. The inlet to the manifold was connected to a pressurized air supply so that each sensor was supplied with the same pressure. Pressure was controlled using a 200 kPa "Druck PACE 6000" calibrated controller with an uncertainty of ±20 Pa.

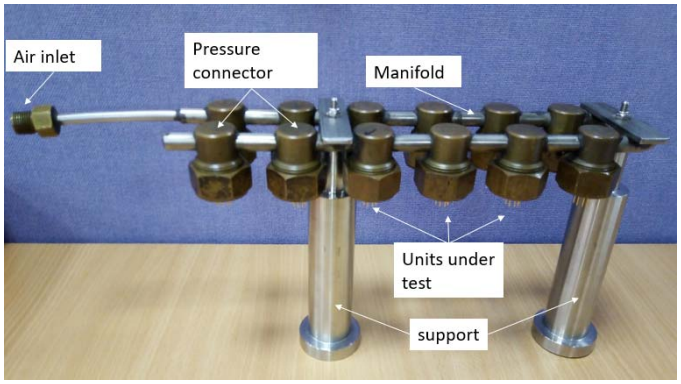

Fig. 3 Photograph of the sensors mounted on the manifold

The bridge output and diode voltages were measured throughout the tests by connecting electrical leads to the housing's feedthrough pins. The populated manifold was then placed in a Temperature Applied Sciences (TAS) environmental chamber capable of controlling temperature over a range of -50 to 200°C with an uncertainty of ±2°C. The sensors were connected via a 40 channel Keysight data logger to an Aim & Thurlby Thandar Instruments (TTi) 10 V DC power supply and a Keysight 6.5 digit resolution digital voltmeter capable of a ±0.1 µV measurement accuracy. This allowed the recording of the bridge output, diode and supply voltages for every sensor connected to the manifold, as well as the applied pressure. All electrical and pressure control equipment was placed outside the environmental chamber and therefore was subjected to any variations in the laboratory temperature, however an air conditioning unit controlled the ambient temperature and it was assumed that any temperature variation of the measurement equipment would have a negligible effect on the study. It should be noted that humidity was not monitored or controlled during these experiments but was not expected to have any impact on the results.

The units were submitted to three cycles, starting and ending at 25°C, over a 5 to 65°C thermal range and a 50 to 200 kPa pressure range, as shown in Fig. 4 [9]. When the temperature was changed from one set point to another, a 60 min dwell time was allowed for the environmental chamber, the manifold and the units to reach a uniform and stable temperature (within the environmental chamber's accuracy). After the dwell time had elapsed, the pressure was cycled from the lowest pressure (50 kPa) to the highest pressure (200 kPa) up and down once. When the pressure was changed, from one pressure point to another, a 30 s dwell time was allowed for the controller to stabilize the pressure within the manifold within its accuracy capability. After stabilization, the supply, bridge output and diode voltages along with applied pressure were measured. It should be noted that the rates of temperature and pressure changes were not recorded. For the FE configuration only, three further cycles were conducted at two extended temperature ranges of -20 to 80°C and of -40 to 125°C. These results are not presented here as the focus of the study was on the limited temperature range, however as will be discussed, the effect of the extended temperatures on the metallisation were assumed not to impact the AE configuration results due to the stabilisation of the hysteresis.

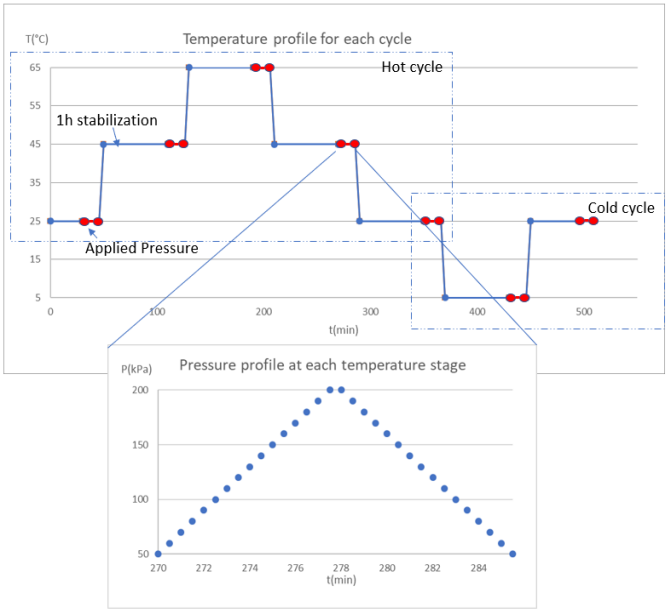

Fig. 4 Temperature and pressure profile for the first cycle

Results

A. Raw data analysis

The raw output for FE packaged sensor #9 subjected to 100 kPa applied pressure throughout three 5 to 65°C thermal cycles is shown in Fig. 5. The vertical axis shows the normalized voltage output, which is the Wheatstone bridge voltage output divided by the bridge supply voltage. For a supply voltage of 5V, the normalized output varies from 12.55 mV/V at 5°C to 11.15 mV/V at 65°C. This represents a thermal variation of -0.023 (mV/V)/°C for a 100 kPa applied pressure. This thermal variation is not desirable from a user's perspective and must be eliminated as much as practically possible. If the raw output was repeatable, one could use a simple linear function to compensate for the negative slope and arrange to have any offset required by the application. At a first glance, the sensor's output seems linear and repeatable over the three cycles, however when zooming in on the individual data points at 45°C for example, it can be seen that the data is not linear and that the data points are not vertically aligned. This highlights that the points were not measured at exactly the same temperature.

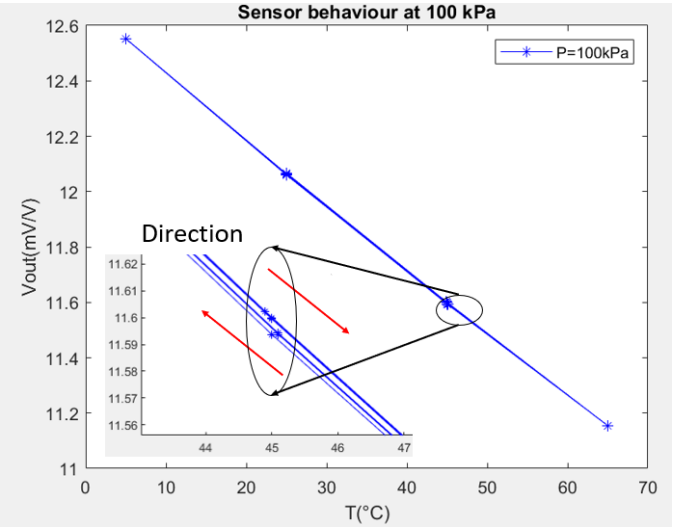

Fig. 5 Normalized bridge voltage output raw data for an FE package at 100 kPa for three 5 to 65°C cycles

B. Fitting data and plotting of hysteresis behaviour

When a constant pressure is applied to a sensor while being thermally cycled, hysteresis for a given temperature can be phenomenologically defined as the difference in the sensor's output between readings obtained when the temperature is increasing and when decreasing. When comparing the output signal for these two halves of the thermal cycle, the data points should ideally be recorded at the exact same temperatures and pressures. However, in practical terms, inaccuracies due to pressure and temperature variation within the measurement system (e.g. Fig. 5) are always present and need to be accounted for. Each sensor is therefore characterized by a unique fitting function relating the normalized output bridge voltage, V_b, to the applied pressure, P, and diode voltage, V_d. This therefore allows interpolation of the measured raw data into fitted data points at exactly the same temperature, whilst also eliminating any repeatable non-linear and temperature dependent behaviour. Thus, it is not the raw data that would be of interest in this study, but the deviation of the fitted data from the raw data which represents the fitting error. It has been found that a third order polynomial function is required to satisfactorily eliminate repeatable thermal non-linearities and that a higher order polynomial provides no further improvement. For a third order polynomial fit, with two inputs and one output, the fitting error, e, between the measured, V_b and fitted, V_{fit} (interpolated) data is:

$$e = V_b - V_{fit} = V_b - \sum_{i,j=0}^{3} a_{ij} V_d^{\,i} P^j \qquad (1)$$

where the a_{ij} are the fitting coefficients obtained using the least squares method. For a fully repeatable unit the error would be zero after the fit function eliminated the non-linear yet repeatable behaviour.

Figure 6 shows the error, i.e. the hysteresis behaviour, for the same FE unit, i.e. #9, during the first test cycle. It should be noted that hysteresis can only be defined for temperature points where the sensor was subjected to the same temperature in both the increasing and decreasing direction e.g. hysteresis for the cycle was defined at 25 and 45°C, but cannot be at the extremes of 5 and 65°C. The hysteresis at 25°C amounted to 7.3 µV/V and to 7.4 µV/V for 45°C. As a worst-case scenario, thermal hysteresis was considered in this paper as the difference between the maximum and minimum error values, irrespective of the temperature points, i.e. in Fig. 6 this would be 7.4 µV/V for the first cycle for a FE sensor at 100 kPa. For a FE sensor having a full-scale (FS) output range of 20 mV/V at 200 kPa, this represents hysteresis values of 365ppm of full-scale output.

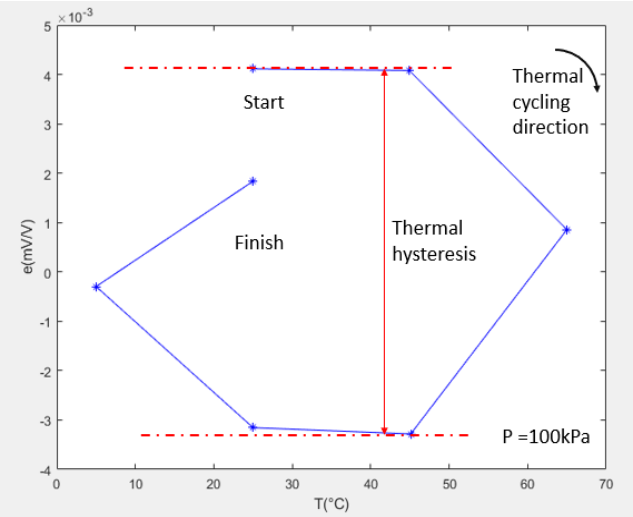

Fig. 6 Fitting error as a function of temperature for a FE packaged sensor (#9) at 100 kPa absolute pressure

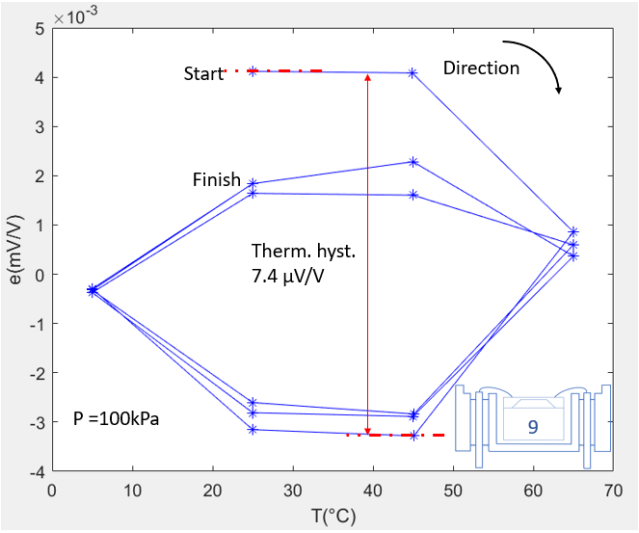

Fig. 7 Thermal cycle fitting error plots for FE test sample #9

Figure 7 shows the hysteresis behaviour for the same FE packaged sensor, #9, for all three thermal cycles. The thermal hysteresis during the second and third cycles was calculated to be 5.2 and 4.7 µV/V respectively. Stabilization into a more repeatable hysteresis loop was evident after three cycles and similar error loops were exhibited for all 10 FE packaged sensors under test. Similar stabilised loops were found to occur for the extended temperature range cycles but with higher hysteresis values. Therefore, the effect of the extended temperatures on the metallisation were assumed not to impact the AE configuration.

Figure 8 shows the hysteresis behaviour over four thermal cycles for the same sensor, #9, after being tested in the FE configuration and then repackaged in the AE configuration. The total hysteresis over the four cycles was calculated to be 21.2 µV/V. The AE configuration shows a distinctly different behaviour to the FE configuration, with a displacement or "ratcheting" of the loops evident. The thermal hysteresis was calculated for each loop, as shown in Fig. 9. There is some evidence that the magnitude of the ratcheting reduced with thermal cycling i.e. from 13.9 to 9.8 µV/V, although four cycles were not sufficient to conclude that motion of the loop would ultimately stabilize. Similar error loops were exhibited for all 5 sensors packaged in the AE configuration.

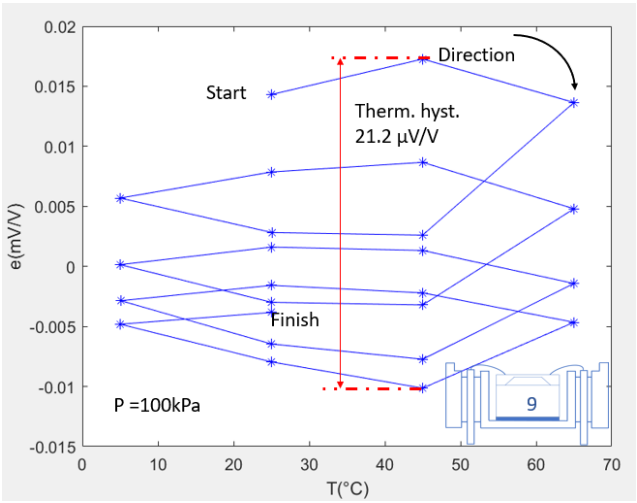

Fig. 8 Thermal cycle fitting error plots for AE test sample #9

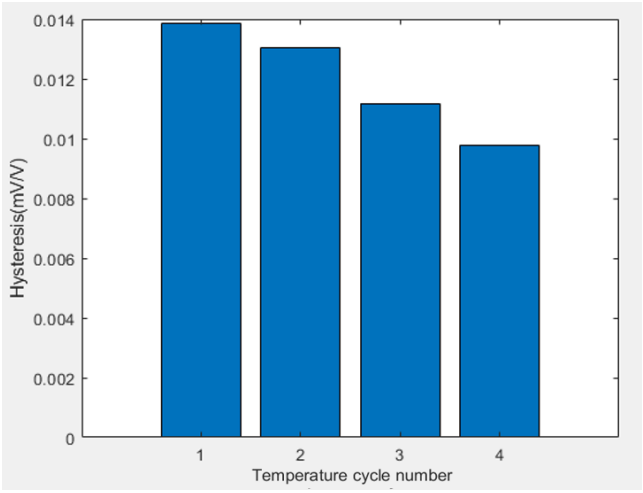

Fig. 9 Thermal hysteresis for SE #9 packaged in the AE configuration subjected to four thermal cycles

Discussion

For the FE configuration, the hysteresis observed could stem from non-repeatable thermal stresses transferred from the packaging elements to the piezoresistors. As the borosilicate glass is CTE matched to silicon and only in contact with the

bottom face of the silicon, it was assumed that the bonding interface does not contribute to the non-repeatability. This leaves the bond pad metallisation and the wire bonds as the remaining packaging elements potentially causing the hysteresis. The metallisation bond pads are sputtered then sintered at a temperature between 350 and 450°C to obtain good ohmic contact. The sensing element is then cooled to room temperature where the 20.7×10^{-6} K^{-1} thermal expansion mismatch between the AlSi1% metallisation and silicon could lead to the development of stresses in the metallisation exceeding the yield limit [9]. Creep induced phenomena during the 60 min dwell period at each temperature of the test cycle is hypothesised to be the principal source of hysteresis in the FE configuration. Another source of hysteresis could stem from the wire bond to bond pad metallisation interface, where there may be changes in the alignment of the AlSi1% grains with thermal cycling [10]. Although the number of cycles is not high, the stabilization of the error loops is believed to come from stress stabilization when subjected to thermal cycling and it seems that just three cycles are sufficient.

The "ratcheting" of the AE configuration is attributed to the inclusion of the additional packaging elements (adhesive attachment to the housing), that were not present in the FE configuration. The effect of the previous cycles that the sensor witnessed during the FE configuration tests were assumed not to cause the ratcheting as the FE hysteresis consistently stabilised. As similar stabilised loops were found for the extended temperature ranges, the effect of these on the metallisation were also assumed not to impact the AE configuration.

The stainless steel housing is unlikely to exhibit any non-linear behaviour at the temperatures and stresses encountered here. The ratcheting behaviour was therefore assumed to only be due to the effect of the adhesive as it is a polymeric material, which may experience visco-elastic and visco-plastic deformation at relatively modest stress levels. The 132×10^{-6} K^{-1} thermal expansion mismatch between the glass and adhesive could generate sufficient stresses to cause hysteresis. Furthermore, the high temperature phases of the thermal cycling could progressively increase the degree of cure within the adhesive and lead to the ratcheting effect. It has not yet been evaluated whether the combination of temperatures and stresses are likely to be in the viscoelastic or plastic regime of the adhesive. Viscoelastic deformation of the adhesive leads to time dependent stresses and strains, which would therefore depend on the dwell time at each temperature and rate of temperature change during the test, while any plastic deformation of the adhesive might lead to a shift in yield between cycles, due to kinematic hardening.

Conclusions

During this study focusing on the packaging effects on hysteresis of 200 kPa absolute piezoresistive sensing elements over a 5 to 65°C temperature range, it was found that for the FE configuration the effects of the metallisation led to a stabilisation of the hysteresis loop after three cycles where for the AE configuration the additional effect of the adhesive layer led to a ratcheting effect of the hysteresis loops.

The hypotheses concerning low temperature induced creep in the metallisation and viscoelastic properties within the adhesive remain to be validated by conducting in depth analysis of the material properties of the different packaging elements. Nanoindentation of the bond pad metallisation at a range of temperatures and times, for example, would assist the verification of any creep behaviour. Furthermore, segregating the effect of the metallisation from the effect of the wire bond in the FE configuration would require further experimentation. In relation to the structural adhesive used in the AE configuration, dynamic mechanical analysis could yield interesting results on the creep behaviour of adhesive joints when subjected to loads and temperatures experienced during testing. Finally, it could understandably be argued that three or four thermal cycles are not enough to make long term stability predictions and a study with more cycles, including varying cycle times, could be more conclusive.

Acknowledgments

This work was partly funded by the EPSRC Centre for Doctoral Training in Embedded Intelligence grant number EP/L014998/1.

References

1. C. S. Smith, "Piezoresistance effect in germanium and silicon", Phys. Rev., vol. 94, no. 1, pp. 42–49, Apr. 1954.
2. O. N. Tufte and E. L. Stelzer, "Piezoresistive Properties of Silicon Diffused Layers", *J. Appl. Phys.*, vol. 34, no. 2, pp. 313–318, 1963.
3. M. A. Hopcroft, W. D. Nix and T. W. Kenny, "What is the Young's modulus of silicon?", J. Microelectromechanical Syst., vol. 19, no. 2, pp. 229–238, 2010.
4 A. A. Barlian, W. Park, J. R. Mallon, A. J. Rastegar and B. L. Pruitt, "Review: Semiconductor Piezoresistance for Microsystems", Proc. IEEE, vol. 97, no. 3, 2009.
5 M. A. Fraga and L. L. Koberstein, "An overview on the modeling of silicon piezoresistive pressure microsensors", *Workshop Eng. Appl. (WEA), Bogota, Columbia, 2-4 May 2012*, no. 1, pp. 12–17.
6 R. H. Krondorfer and Y. K. Kim, "Packaging effect on MEMS pressure sensor performance", *IEEE Trans. Components Packag. Technol.*, vol. 30, no. 2, pp. 285–293, 2007.
7 Y. Liu, H. Wang, W. Zhao, H. Qin and X. Fang, "Thermal-Performance Instability in Piezoresistive Sensors: Inducement and Improvement", *Sensors*, vol. 16, no. 12, p. 23, Nov. 2016.
8 Y. Kanda, "A Graphical Representation Of The Piezoresistance Coefficients In Silicon", *IEEE Trans. Electron Devices*, vol. 29, no. 1, pp. 64–70, 1982.
9 Y. Hamid, D. A. Hutt, D. C. Whalley and R. Craddock, "Effect of Thin Film Interconnect Inelasticity on MEMS Pressure Sensor Hysteresis", *Proceedings of the 5th Int. Conf. Sensors Electron. Instrum. Adv.*, Tenerife, Spain 25-27 September 2019, pp. 3–4, 2019.
10 G. Khatibi, B. Weiss, J. Bernardi and S. Schwarz, "Microstructural investigation of interfacial features in Al wire bonds", *J. Electron. Mater.*, vol. 41, no. 12, pp. 3436–3446, 2012.